

Article

# Growth and Photocatalytic Properties of Gallium Oxide Films Using Chemical Bath Deposition

Che-Yuan Yeh <sup>1,†</sup>, Yi-Man Zhao <sup>1,2,†</sup>, Hui Li <sup>1,2</sup>, Fei-Peng Yu <sup>3</sup>, Sam Zhang <sup>2,\*</sup> and Dong-Sing Wu <sup>1,4,\*</sup> 

<sup>1</sup> Department of Materials Science and Engineering, National Chung Hsing University, No. 145, Xingda Rd., Taichung 40227, Taiwan; w105066022@mail.nchu.edu.tw (C.-Y.Y.); zym19920609@163.com (Y.-M.Z.); lihui@kaist.ac.kr (H.L.)

<sup>2</sup> Center for Advanced Thin Films and Devices, School of Materials and Energy, Southwest University, No. 2, Tiansheng Rd., Chongqing 400715, China

<sup>3</sup> Department of Materials Science and Engineering, Da-Yeh University, No. 168, University Rd., Changhua 51591, Taiwan; pon.pon@ms25.url.com.tw

<sup>4</sup> Innovation and Development Center of Sustainable Agriculture, National Chung Hsing University, No. 145, Xingda Rd., Taichung 40227, Taiwan

\* Correspondence: SamZhang@swu.edu.cn (S.Z.); dsw@nchu.edu.tw (D.-S.W.)

† These authors contributed equally to this work.

Received: 4 October 2019; Accepted: 25 October 2019; Published: 27 October 2019



**Abstract:** Gallium oxide ( $\text{Ga}_2\text{O}_3$ ) thin films were fabricated on glass substrates using a combination of chemical bath deposition and post-annealing process. From the field-emission scanning electron microscopy and x-ray diffraction results, the GaOOH nanorods precursors with better crystallinity can be achieved under higher concentrations ( $\geq 0.05$  M) of gallium nitrate ( $\text{Ga}(\text{NO}_3)_3$ ). It was found that the GaOOH synthesized from lower  $\text{Ga}(\text{NO}_3)_3$  concentration did not transform into  $\alpha$ - $\text{Ga}_2\text{O}_3$  among the annealing temperatures used (400–600 °C). Under higher  $\text{Ga}(\text{NO}_3)_3$  concentrations ( $\geq 0.05$  M) with higher annealing temperatures ( $\geq 500$  °C), the GaOOH can be transformed into the  $\text{Ga}_2\text{O}_3$  film successfully. An  $\alpha$ - $\text{Ga}_2\text{O}_3$  sample synthesized in a mixed solution of 0.075 M  $\text{Ga}(\text{NO}_3)_3$  and 0.5 M hexamethylenetetramine exhibited optimum crystallinity after annealing at 500 °C, where the  $\alpha$ - $\text{Ga}_2\text{O}_3$  nanostructure film showed the highest aspect ratio of 5.23. As a result, the photodegradation efficiencies of the  $\alpha$ - $\text{Ga}_2\text{O}_3$  film for the methylene blue aqueous solution can reach 90%.

**Keywords:**  $\text{Ga}_2\text{O}_3$ ; GaOOH; chemical bath deposition; photocatalytic property

## 1. Introduction

Environmental protection, especially against water pollution, has generated public interest in recent years, and the application of nanotechnology in this field has become a hot topic. Photocatalysis using natural sunlight as a clean energy source, has been extensively studied for environmental remediation since its discovery [1–4]. Methylene blue (MB), a common dye, has been widely used for the commercial products such as the dyeing paper, linen, silk fabric, bamboo, wood, etc. The discharge of untreated MB into the wastewater can lead to serious pollution problems, making degradation and decolorization of MB is one of the important targets of dyeing wastewater treatment [5,6].

Metal oxides, such as titanium dioxide, zinc oxide, and gallium oxide ( $\text{Ga}_2\text{O}_3$ ), are considered promising for photocatalytic applications due to their excellent physical and chemical properties [7–11]. Among these metal oxides,  $\text{Ga}_2\text{O}_3$ , with various polymorphs ( $\alpha$ -,  $\beta$ -,  $\gamma$ -,  $\delta$ -, and  $\epsilon$ -) can be synthesized at different temperatures [12,13]. Gallium oxides, which have wide bandgap ranging from 4.2 to 4.9 eV, are particularly important semiconductor materials [11,14]. The  $\text{Ga}_2\text{O}_3$  material can be used for various device applications, such as gas sensors [15], catalysis [16], power and high voltage electronic

devices [13] because it has unique conductive properties and is electrically and thermodynamically stable [17–19]. Various polymorphs of Ga<sub>2</sub>O<sub>3</sub> as the photocatalysts in the degradation of organic dyes have been studied previously [11,20–22]. Reddy et al. [11] have reported that the photodegradation efficiencies of α-Ga<sub>2</sub>O<sub>3</sub> and β-Ga<sub>2</sub>O<sub>3</sub> nanorods for the rhodamine B aqueous solution were 62% and 79%, respectively. The photocatalytic activity of α-Ga<sub>2</sub>O<sub>3</sub> in the malachite green degradation was studied by Rodríguez et al. [20]. Zhao et al. [21], have demonstrated that the photodegradation efficiency of β-Ga<sub>2</sub>O<sub>3</sub> nanorods in the perfluorooctanoic acid can reach 98.8%. In addition, the photocatalytic activity of the γ-Ga<sub>2</sub>O<sub>3</sub> in rhodamine 590 degradation has also been investigated by Jin et al. [22].

Recently, various methods have been used to synthesize Ga<sub>2</sub>O<sub>3</sub>, including hydrothermal techniques [11,23], microwave-assisted hydrothermal methods [21], sol-gel methods [24], spray pyrolysis processes [25], and chemical vapor deposition [26]. The advantages of CBD for the synthesis of metal oxide thin films are based on the relatively low cost and convenience for deposition over a large area [27]. However, there are very few reports on the synthesis of Ga<sub>2</sub>O<sub>3</sub> thin films via CBD. In this study, the Ga<sub>2</sub>O<sub>3</sub> thin films were synthesized on the glass substrates using CBD with various post annealing treatments. The chemistry of the synthesis process can be summarized as follows [20,28–30]:



## 2. Experimental

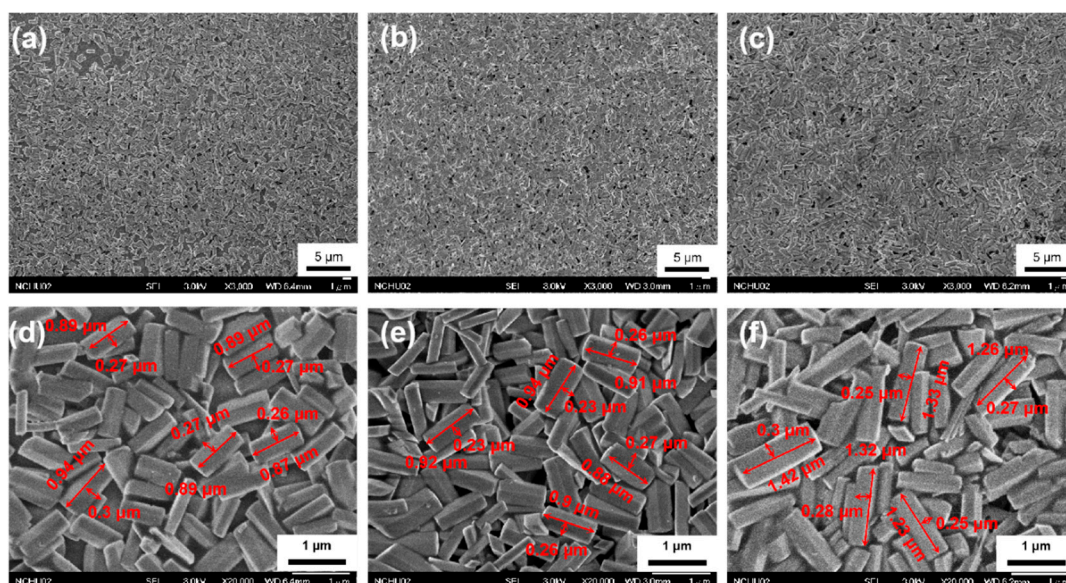
Ga<sub>2</sub>O<sub>3</sub> thin films were prepared on glass substrates using CBD. Analytical grade gallium (III) nitrate hydrate (Ga(NO<sub>3</sub>)<sub>3</sub>·nH<sub>2</sub>O, 99.9%) and hexamethylenetetramine (HMT, 99.9%) were used as starting materials. The glass substrates were cleaned with acetone, methanol, and 10% hydrofluoric acid for 10 min respectively, then rinsed with deionized (DI) water. Three growth solutions were prepared by dissolving 0.025 mol, 0.05 mol, or 0.075 mol Ga(NO<sub>3</sub>)<sub>3</sub> and 0.5 mol HMT in 1 L of DI water. To obtain the GaOOH precursor, each aqueous solution was placed in a beaker with a glass substrate and vigorously stirred at 500 rpm with a magnetic stirrer for 5 h at 95 °C. The precursor was then dried at 70 °C for 5 min and allowed to cool naturally to room temperature. The as-prepared GaOOH thin films were annealed in a furnace tube at either 400 °C, 500 °C, or 600 °C for 3 h to form Ga<sub>2</sub>O<sub>3</sub> thin films.

The crystal structures of the as-prepared samples were characterized using a high resolution X-ray diffraction system (HR-XRD, X'Pert Pro MRD, PANalytical, Almelo, Nederland). A JSM-6700F field-emission scanning electron microscope (FE-SEM, JEOL, Tokyo, Japan) equipped with an energy dispersive spectrometer (EDS) was used to analyze the morphologies of the samples and their elemental distributions. FT-IR spectra were collected in the range from 4000 to 500 cm<sup>-1</sup> with a Vertex 80v Fourier transform infrared spectrometer (Bruker, Billerica, Massachusetts, MA, USA). The photocatalytic properties of the Ga<sub>2</sub>O<sub>3</sub> thin films in aqueous MB solutions were evaluated during and after irradiation under an 8 W UV lamp at wavelengths from 100 to 280 nm. Thin films with dimensions of 1 cm × 1 cm were first placed in aqueous solutions containing 5 ppm MB. The solutions were then irradiated for 5 h at room temperature in an otherwise dark environment. Photodegradation efficiency was determined through UV-visible spectrophotometric analysis (U3010, Hitachi, Tokyo, Japan)

## 3. Results and Discussion

The FE-SEM images of the GaOOH nanostructures obtained via CBD at various Ga(NO<sub>3</sub>)<sub>3</sub> concentrations are shown in Figure 1, where the length, width, and the aspect ratio of at least eight GaOOH nanorods were measured. It was found that the Ga(NO<sub>3</sub>)<sub>3</sub> concentration significantly

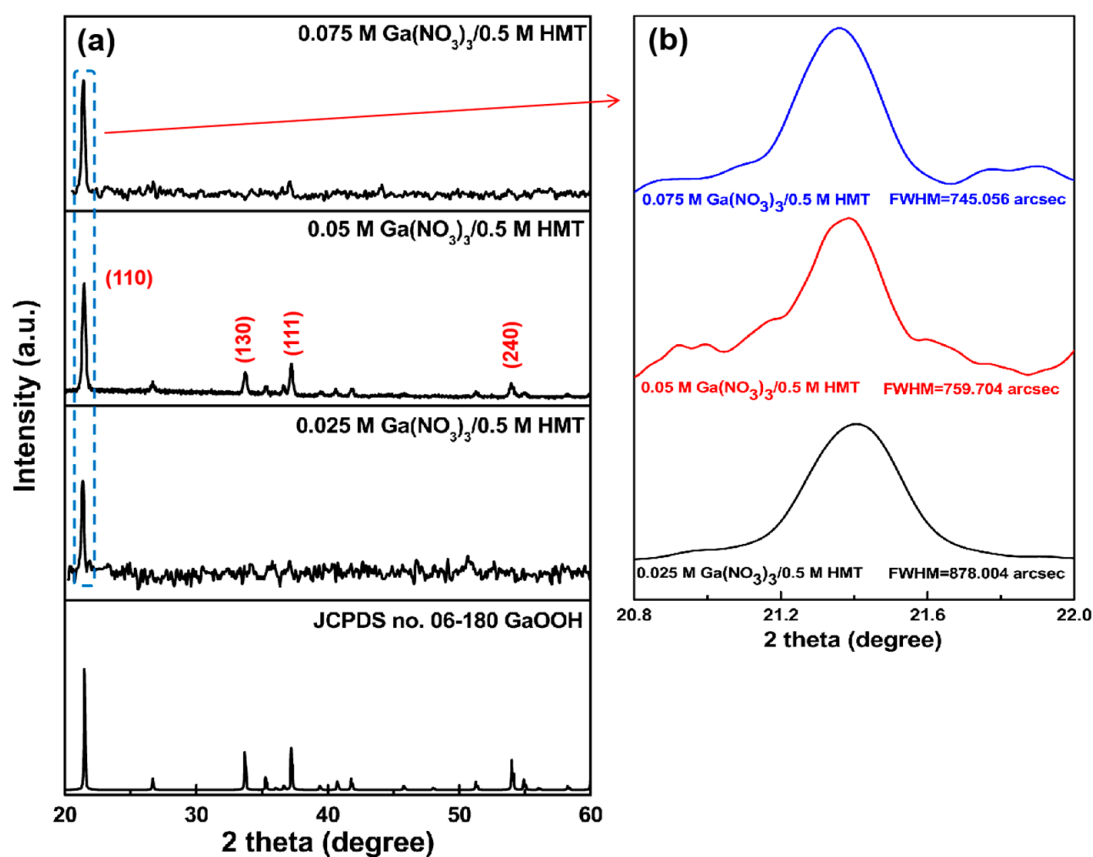
influenced the synthesis of GaOOH nanorods and the formation of Ga<sub>2</sub>O<sub>3</sub> thin films during the annealing process. The GaOOH crystalline quality increased as the Ga(NO<sub>3</sub>)<sub>3</sub> concentration increased from 0.025 M (Figure 1a,d) to 0.075 M (Figure 1c,f). The average length, width and the aspect ratio of the GaOOH nanorods prepared from 0.025 M Ga(NO<sub>3</sub>)<sub>3</sub> were 0.88  $\mu\text{m}$ , 0.27  $\mu\text{m}$  and 3.23, respectively (Figure 1d). The average length, width and the aspect ratio of the GaOOH nanorods prepared from 0.05 M Ga(NO<sub>3</sub>)<sub>3</sub> were 0.92  $\mu\text{m}$ , 0.25  $\mu\text{m}$  and 3.76, respectively (Figure 1e). When the Ga(NO<sub>3</sub>)<sub>3</sub> concentration increased to 0.075 M, the average length, width and the aspect ratio of the GaOOH nanorods increased to 1.24  $\mu\text{m}$ , 0.25  $\mu\text{m}$  and 5.06, respectively (Figure 1f). These indicated that the higher concentration of Ga(NO<sub>3</sub>)<sub>3</sub> yielded the GaOOH nanorods with better crystallinity.



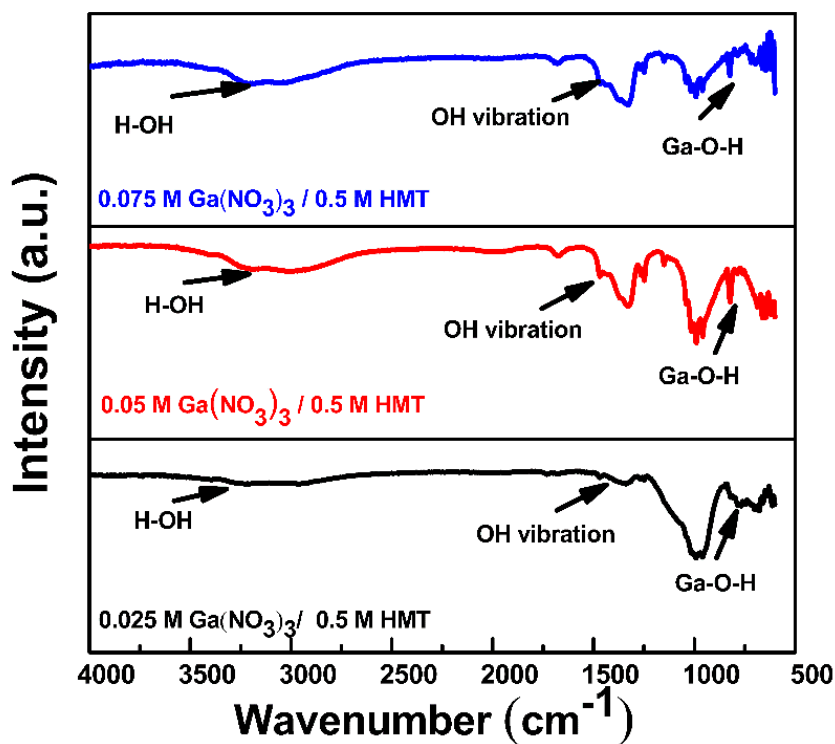
**Figure 1.** FE-SEM images of GaOOH prepared from Ga(NO<sub>3</sub>)<sub>3</sub> at concentrations ranging from 0.025 M to 0.075 M: (a) 0.025 M; (b) 0.05 M; (c) 0.075 M. Their corresponding enlarged micrographs are shown in (d–f), respectively.

Figure 2a shows the XRD pattern of the as-prepared GaOOH obtained at each Ga(NO<sub>3</sub>)<sub>3</sub> concentration. The full width at half maximum (FWHM) of each (110) crystal plane diffraction peak was calculated from XRD data as shown in Figure 2b. The XRD patterns indicated the as-prepared GaOOH had an orthorhombic structure (JCPDS no. 01–180). The sharp diffraction peak of the (110) crystal plane appeared at ( $2\theta$ ) 21.4° in the pattern of each sample. This indicated that GaOOH crystal growth proceeded preferentially in the [001] direction at each Ga(NO<sub>3</sub>)<sub>3</sub> concentration. The diffraction peaks of the (130), (111), and (240) crystal planes of GaOOH were observed at ( $2\theta$ ) 33.7°, 37.2°, and 54.02°, respectively. The peaks at 21.4° in the patterns of GaOOH nanorods prepared using 0.025 M, 0.05 M, and 0.075 M Ga(NO<sub>3</sub>)<sub>3</sub> had FWHMs of 878, 759.7, and 745.1 arcsec, respectively (Figure 2b). The FWHM of this peak was related to the crystallinity of the GaOOH nanorods and indicated that the crystallinity of the nanorods prepared with 0.075 M Ga(NO<sub>3</sub>)<sub>3</sub> was higher than that of the other GaOOH samples. The XRD results agreed well with the crystallinity trend of the GaOOH nanorods deposited from various Ga(NO<sub>3</sub>)<sub>3</sub> concentrations as presented in Figure 1.

An FTIR spectra of the as-prepared GaOOH nanorods synthesized at each Ga(NO<sub>3</sub>)<sub>3</sub> concentration is shown in Figure 3. It is known that the peak at  $\sim 3222\text{ cm}^{-1}$  in the FTIR spectra of GaOOH nanorods was assigned to the H-OH stretching vibration, and the stretching vibration of O–H bonds was observed around  $1323\text{ cm}^{-1}$  due to the adsorption of water molecules [11,31]. The peak at  $\sim 750\text{ cm}^{-1}$  was assigned to the Ga-O-H stretching vibration [20]. It is worthy to mention that the Ga-O-H bond will be enhanced and shifted from  $\sim 750$  to  $\sim 820\text{ cm}^{-1}$  as the GaOOH content increased, [31,32]. This confirmed that the GaOOH nanostructure thin films were successfully grown on the glass substrates via CBD.



**Figure 2.** (a) XRD patterns of as-prepared GaOOH nanorods obtained from Ga(NO<sub>3</sub>)<sub>3</sub> at concentrations of 0.025 M, 0.05 M, and 0.075 M. (b) FWHMs of the GaOOH (110) crystal plane diffraction peaks shown in (a).



**Figure 3.** FTIR spectra of GaOOH prepared from Ga(NO<sub>3</sub>)<sub>3</sub> at various concentrations.

Figure 4 shows the XRD patterns of Ga<sub>2</sub>O<sub>3</sub> in the films after annealing for 3 h at various temperatures from 400 to 600 °C. As shown in Figure 4a, the α-Ga<sub>2</sub>O<sub>3</sub> polymorph (JCPDS no. 06–0503) was not indicated in any of the samples annealed at 400 °C. Possibly, the GaOOH could not change to α-Ga<sub>2</sub>O<sub>3</sub> at such a low temperature [12]. It was also found that the GaOOH synthesized from 0.025 M Ga(NO<sub>3</sub>)<sub>3</sub> did not transform into α-Ga<sub>2</sub>O<sub>3</sub> among these annealing temperatures. However, the transformation of as-prepared GaOOH into orthorhombic α-Ga<sub>2</sub>O<sub>3</sub> occurred during annealing at 500 and 600 °C. The sharp diffraction peaks of the (104) and (110) α-Ga<sub>2</sub>O<sub>3</sub> crystal planes were observed at (2θ) 33.78° and 36.03°, respectively. Table 1 shows the FWHM data of the (104) α-Ga<sub>2</sub>O<sub>3</sub> diffraction peaks obtained from 500 and 600 °C-annealed GaOOH samples with 0.05 and 0.075 M Ga(NO<sub>3</sub>)<sub>3</sub> concentrations. Obviously, the CBD-GaOOH sample with 0.075 M Ga(NO<sub>3</sub>)<sub>3</sub> concentration and post thermal treatment at 500 °C can result in higher crystallinity of α-Ga<sub>2</sub>O<sub>3</sub>.

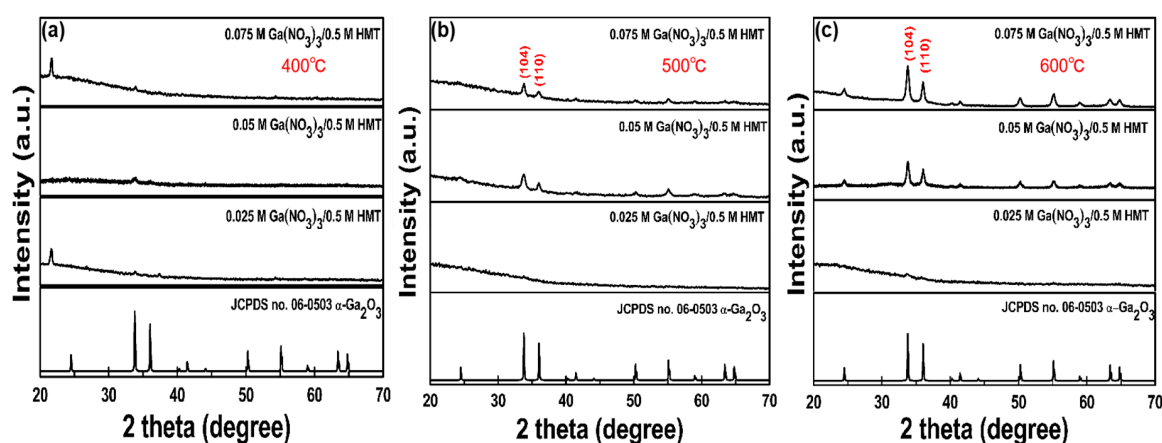
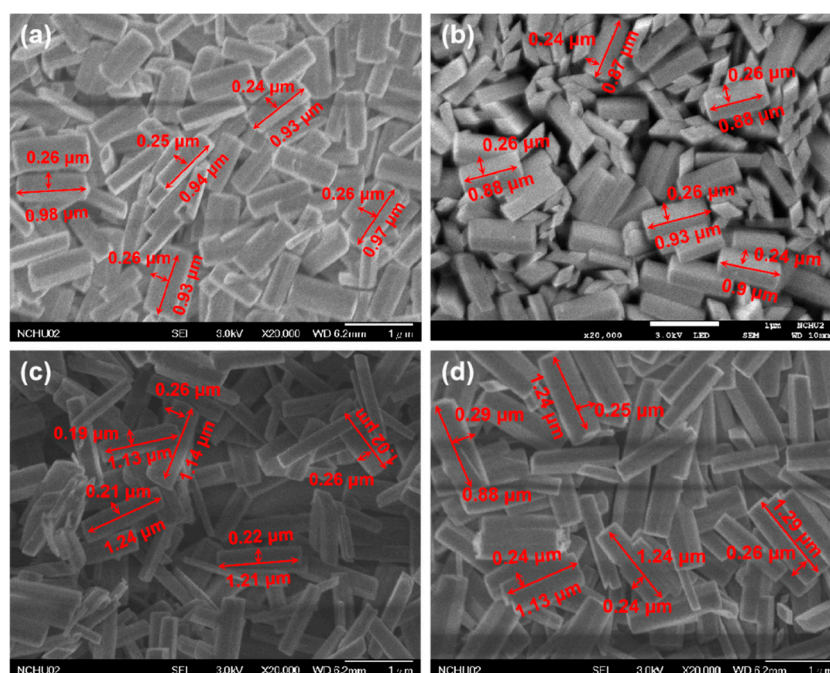


**Figure 4.** XRD patterns of Ga<sub>2</sub>O<sub>3</sub> obtained from thermal-treated GaOOH samples for 3 h at various temperatures (a) 400 °C, (b) 500 °C and (c) 600 °C.

**Table 1.** The FWHM data of (104) α-Ga<sub>2</sub>O<sub>3</sub> diffraction peaks obtained from post-annealed GaOOH samples with 0.05 and 0.075 M Ga(NO<sub>3</sub>)<sub>3</sub> concentrations.

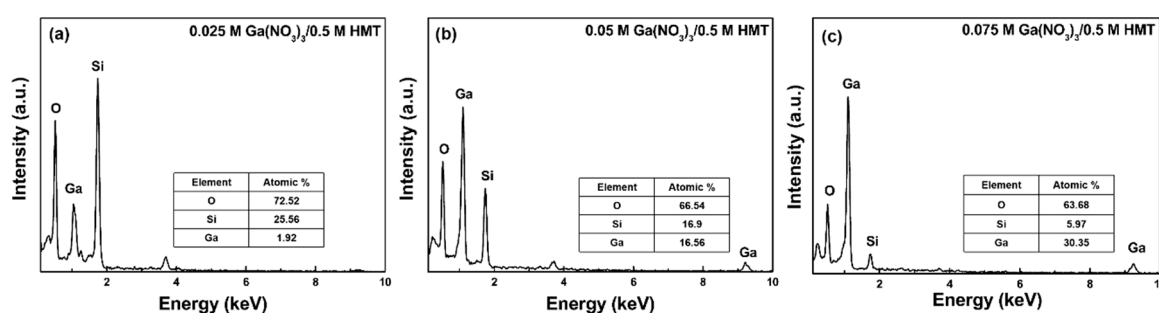
Annealed Temperature	0.05 M Ga(NO <sub>3</sub> ) <sub>3</sub>	0.075 M Ga(NO <sub>3</sub> ) <sub>3</sub>
500 °C	2153.5 arcsec	1567.4 arcsec
600 °C	1715 arcsec	1700.6 arcsec

Figure 5 shows the corresponding FE-SEM micrograph of the α-Ga<sub>2</sub>O<sub>3</sub> sample as tabulated in Table 1. After annealing at 500 °C, the average length, width and the aspect ratio of the Ga<sub>2</sub>O<sub>3</sub> nanorods obtained from CBD-GaOOH with 0.05 M Ga(NO<sub>3</sub>)<sub>3</sub> were 0.94 μm, 0.26 μm and 3.63, respectively (Figure 5a). When the annealing temperature increased to 600 °C, the average length, width and the aspect ratio of the Ga<sub>2</sub>O<sub>3</sub> nanorods were 0.89 μm, 0.26 μm, and 3.45, respectively (Figure 5b). Besides, the average length, width and the aspect ratio of the Ga<sub>2</sub>O<sub>3</sub> nanorods obtained from 500 °C-annealed GaOOH with 0.075 M Ga(NO<sub>3</sub>)<sub>3</sub> were 1.16 μm, 0.23 μm and 5.23, respectively (Figure 5c). When the annealing temperature increased to 600 °C, the average length, width and the aspect ratio of the Ga<sub>2</sub>O<sub>3</sub> nanorods were 1.22 μm, 0.26 μm, and 4.68, respectively (Figure 5d). Here, all the data of length, width, and the aspect ratio shown in the micrographs were measured at least eight times. It becomes clear that the higher annealing temperature (i.e., 600 °C) will lead to the slight decrease in the aspect ratio of Ga<sub>2</sub>O<sub>3</sub> nanorods. As a result, these nanorods were tightly packed together.



**Figure 5.** FE-SEM  $\text{Ga}_2\text{O}_3$  obtained after annealing  $\text{GaOOH}$  at 500 °C: (a) 0.05 M; (c) 0.075 M; and 600 °C: (b) 0.05 M; (d) 0.075 M.

The elemental compositions of the annealed samples were analyzed via EDS. The EDS spectra of samples prepared using  $\text{Ga}(\text{NO}_3)_3$  at various concentrations after annealing at 500 °C are shown in Figure 6. The Si peaks in the EDS spectra were attributed to silicon in the glass substrates. The at.% of Ga in the sample prepared from 0.025 M  $\text{Ga}(\text{NO}_3)_3$  was only 1.92% (Figure 6a). When the  $\text{Ga}(\text{NO}_3)_3$  concentration increased to 0.05 M, the content of Ga atoms in the sample increased to 16.56% (Figure 6b). Moreover, the at.% of Ga in the sample prepared from 0.075 M  $\text{Ga}(\text{NO}_3)_3$  was 30.35% (Figure 6c). From the XRD results as described in Figure 4, the CBD- $\text{GaOOH}$  prepared under the lower concentration (0.025 M) cannot be transformed into the  $\alpha\text{-Ga}_2\text{O}_3$  regardless of the annealing temperature. It may be due to the fact that the 0.025 M  $\text{Ga}(\text{NO}_3)_3$  cannot provide enough Ga content to transform into  $\alpha\text{-Ga}_2\text{O}_3$ .



**Figure 6.** EDS spectra of annealed samples synthesized using (a) 0.025 M  $\text{Ga}(\text{NO}_3)_3$ , (b) 0.05 M  $\text{Ga}(\text{NO}_3)_3$  and (c) 0.075 M  $\text{Ga}(\text{NO}_3)_3$ . The samples were annealed for 3 h at 500 °C.

The photocatalytic properties of the  $\alpha\text{-Ga}_2\text{O}_3$  thin films in the MB solutions were examined under irradiation with UV light. The  $\text{Ga}_2\text{O}_3$  shows the photocatalytic activity under deep-UV absorption owing to its high bandgap. In general, when the photon was absorbed into photocatalyst, the electron-hole pairs generated on the surface of  $\text{Ga}_2\text{O}_3$  were used to the degradation of the MB solution. After interacting with aqueous media, these electrons and holes generate hydroxyl ions, which play the significant role in the degradation process. These hydroxyl ions have strong oxidation capabilities as they can mineralize most of organic compounds. Moreover, the photocatalytic activities

intimately depend on the crystallinity and surface area. From the XRD (Figure 4) and FWHMs analyses (Table 1), the good crystallinity of  $\alpha$ -Ga<sub>2</sub>O<sub>3</sub> sample prepared using 0.075 M Ga(NO<sub>3</sub>)<sub>3</sub> can bring the stable photocatalytic properties as compared with those of the other  $\alpha$ -Ga<sub>2</sub>O<sub>3</sub> samples. The calculated constant reaction rates of MB photodegradation by Ga<sub>2</sub>O<sub>3</sub> in the solutions ( $C/C_0$ ) are plotted as a function of UV irradiation time in Figure 7.  $C_0$  is the initial MB concentration in solution, and  $C$  is the MB concentration in the UV-irradiated solution. The rates of MB self-degradation in solutions without the catalyst are shown for comparison. Absorbance by MB was monitored at 664 nm [33]. After 5 h of UV irradiation, 82% of the MB was photodegraded by  $\alpha$ -Ga<sub>2</sub>O<sub>3</sub> obtained from GaOOH prepared from 0.05 M Ga(NO<sub>3</sub>)<sub>3</sub> after annealing at 500 °C (Figure 7b). Photodegradation by  $\alpha$ -Ga<sub>2</sub>O<sub>3</sub> obtained from the GaOOH sample prepared using 0.075 M Ga(NO<sub>3</sub>)<sub>3</sub> after annealing at 500 °C was particularly efficient. After UV irradiation for 5 h, 90% of the MB had been photodegraded by the catalyst (Figure 7c). As shown in Figure 7a, only 29% of the MB was photodegraded by the sample obtained from GaOOH prepared using 0.025 M Ga(NO<sub>3</sub>)<sub>3</sub>. Based on the XRD results (Figure 4), its low photodegradation efficiency may have been due to the lack of GaOOH transformation into  $\alpha$ -Ga<sub>2</sub>O<sub>3</sub>. The photodegradation efficiencies of  $\alpha$ -Ga<sub>2</sub>O<sub>3</sub> samples obtained after annealing at 500 °C were higher than those of  $\alpha$ -Ga<sub>2</sub>O<sub>3</sub> obtained after annealing at 600 °C. This may have been due to the higher the aspect ratio of the  $\alpha$ -Ga<sub>2</sub>O<sub>3</sub> annealed at 500 °C, which can lead to more surface area under the process of the degradation of the MB solution. The photocatalytic properties of  $\alpha$ -Ga<sub>2</sub>O<sub>3</sub> observed during the degradation of MB suggested it held promise for environmental remediation applications.

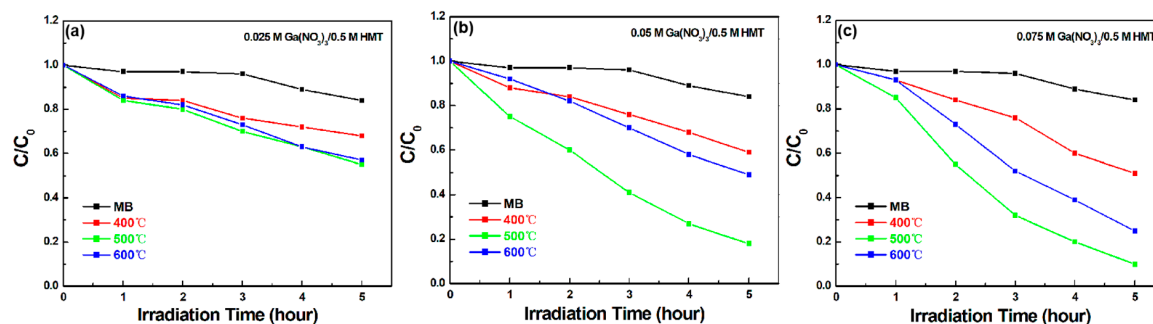


**Figure 7.** Calculated constant reaction rate of MB photodegradation ( $C/C_0$ ) by Ga<sub>2</sub>O<sub>3</sub> plotted as a function of UV irradiation time. The Ga<sub>2</sub>O<sub>3</sub> samples were obtained following annealing of GaOOH prepared at Ga(NO<sub>3</sub>)<sub>3</sub> concentrations of (a) 0.025 M, (b) 0.05 M and (c) 0.075 M.

#### 4. Conclusions

GaOOH thin films were successfully grown on glass substrates via CBD at 95 °C. The as-prepared GaOOH thin films were annealed for 3 h at either 400 °C, 500 °C, or 600 °C to convert GaOOH into thin films of  $\alpha$ -Ga<sub>2</sub>O<sub>3</sub>, and the crystal structures and elemental compositions were confirmed through the XRD and EDS analysis, respectively. Nanocrystalline  $\alpha$ -Ga<sub>2</sub>O<sub>3</sub> films were obtained from GaOOH prepared at Ga(NO<sub>3</sub>)<sub>3</sub> concentrations at or above 0.05 M after annealing at 500 °C or 600 °C. The  $\alpha$ -Ga<sub>2</sub>O<sub>3</sub> sample obtained after annealing GaOOH prepared at a Ga(NO<sub>3</sub>)<sub>3</sub> concentration of 0.075 M photodegraded 90% of the MB in a solution irradiated under a UV lamp for 5 h. These results suggest that  $\alpha$ -Ga<sub>2</sub>O<sub>3</sub> thin films can be very useful alternatives for the photocatalytic degradation of dyes during wastewater treatment.

**Author Contributions:** Conceptualization and supervision, D.-S.W.; methodology, C.-Y.Y.; H.L. and F.-P.Y.; validation, C.-Y.Y.; data curation, C.-Y.Y. and Y.-M.Z.; writing-review and editing; Y.-M.Z., S.Z. and D.-S.W.

**Funding:** This work was financially supported by the Ministry of Science and Technology of Taiwan under grant No. 108-2221-E-005-028-MY3 and in part by the “Innovation and Development Center of Sustainable Agriculture” from The Featured Areas Research Center Program within the framework of the Higher Education Sprout Project by the Ministry of Education (MOE) in Taiwan. The work at Southwest University was partly supported by Fundamental Research Funds for the Central Universities: SWU118105.

**Acknowledgments:** The authors would like to thank the technical support from Yi-Guo Shang in the Department of Materials Science and Engineering, National Chung Hsing University, Taiwan, especially for the setup of chemical bath deposition and photocatalytic measurement systems.

**Conflicts of Interest:** The authors declare that they have no conflict of interest.

## References

1. Fujishima, A.; Honda, K. Electrochemical Photolysis of Water at a Semiconductor Electrode. *Nature* **1972**, *238*, 37–38. [[CrossRef](#)] [[PubMed](#)]
2. Fujishima, A. Hydrogen Production under Sunlight with an Electrochemical Photocell. *J. Electrochem. Soc.* **1975**, *122*, 1487. [[CrossRef](#)]
3. Djurišić, A.B.; Leung, Y.H.; Ng, A.M.C. Strategies for improving the efficiency of semiconductor metal oxide photocatalysis. *Mater. Horizons* **2014**, *1*, 400. [[CrossRef](#)]
4. Benjwal, P.; Kar, K.K. Simultaneous photocatalysis and adsorption based removal of inorganic and organic impurities from water by titania/activated carbon/carbonized eponocoxy namposite. *J. Environ. Chem. Eng.* **2015**, *3*, 2076–2083. [[CrossRef](#)]
5. Houas, A. Photocatalytic degradation pathway of methylene blue in water. *Appl. Catal. B Environ.* **2001**, *31*, 145–157. [[CrossRef](#)]
6. Lachheb, H.; Puzenat, E.; Houas, A.; Ksibi, M.; Elaloui, E.; Guillard, C.; Herrmann, J.-M. Photocatalytic degradation of various types of dyes (Alizarin S, Crocein Orange G, Methyl Red, Congo Red, Methylene Blue) in water by UV-irradiated titania. *Appl. Catal. B Environ.* **2002**, *39*, 75–90. [[CrossRef](#)]
7. Tan, L.-L.; Ong, W.-J.; Chai, S.-P.; Goh, B.T.; Mohamed, A.R. Visible-light-active oxygen-rich TiO<sub>2</sub> decorated 2D graphene oxide with enhanced photocatalytic activity toward carbon dioxide reduction. *Appl. Catal. B Environ.* **2015**, *179*, 160–170. [[CrossRef](#)]
8. Liu, L.; Gao, F.; Zhao, H.; Li, Y. Tailoring Cu valence and oxygen vacancy in Cu/TiO<sub>2</sub> catalysts for enhanced CO<sub>2</sub> photoreduction efficiency. *Appl. Catal. B Environ.* **2013**, *134*, 349–358. [[CrossRef](#)]
9. Núñez, J.; O’Shea, V.A.D.L.P.; Jana, P.; Coronado, J.M.; Serrano, D.P.; O’Shea, V.A.D.L.P. Effect of copper on the performance of ZnO and ZnO<sub>1-x</sub>N<sub>x</sub> oxides as CO<sub>2</sub> photoreduction catalysts. *Catal. Today* **2013**, *209*, 21–27. [[CrossRef](#)]
10. Pan, Y.-X.; Sun, Z.-Q.; Cong, H.-P.; Men, Y.-L.; Xin, S.; Song, J.; Yu, S.-H. Photocatalytic CO<sub>2</sub> reduction highly enhanced by oxygen vacancies on Pt-nanoparticle-dispersed gallium oxide. *Nano Res.* **2016**, *9*, 1689–1700. [[CrossRef](#)]
11. Reddy, L.S.; Ko, Y.H.; Yu, J.S. Hydrothermal Synthesis and Photocatalytic Property of β-Ga<sub>2</sub>O<sub>3</sub> Nanorods. *Nanoscale Res. Lett.* **2015**, *10*, 364. [[CrossRef](#)] [[PubMed](#)]
12. Roy, R.; Hill, V.G.; Osborn, E.F. Polymorphism of Ga<sub>2</sub>O<sub>3</sub> and the System Ga<sub>2</sub>O<sub>3</sub>—H<sub>2</sub>O. *J. Am. Chem. Soc.* **1952**, *74*, 719–722. [[CrossRef](#)]
13. Stepanov, S.I.; Nikolaev, V.I.; Bougrov, V.E.; Romanov, A.E. Gallium oxide: Properties and applications—a review. *Mater. Sci.* **2016**, *44*, 63–86.
14. Liu, X.; Qiu, G.; Zhao, Y.; Zhang, N.; Yi, R. Gallium oxide nanorods by the conversion of gallium oxide hydroxide nanorods. *J. Alloys Compd.* **2007**, *439*, 275–278. [[CrossRef](#)]
15. Pilliadugula, R.; Krishnan, N. Gas sensing performance of GaOOH and β-Ga<sub>2</sub>O<sub>3</sub> synthesized by hydrothermal method: A comparison. *Mater. Res. Express* **2019**, *6*, 025027. [[CrossRef](#)]
16. Nakagawa, K.; Kajita, C.; Okumura, K.; Ikenaga, N.-O.; Nishitani-Gamo, M.; Ando, T.; Kobayashi, T.; Suzuki, T. Role of Carbon Dioxide in the Dehydrogenation of Ethane over Gallium-Loaded Catalysts. *J. Catal.* **2001**, *203*, 87–93. [[CrossRef](#)]
17. Kuperberg, J.M.; Réti, F.; Miró, J.; Herndon, R.C.; Hajnal, Z.; Kiss, G.; Deák, P. Role of oxygen vacancy defect states in the n-type conduction of β-Ga<sub>2</sub>O<sub>3</sub>. *J. Appl. Phys.* **1999**, *86*, 3792–3796.
18. Wu, X.; Song, W.; Huang, W.; Pu, M.; Zhao, B.; Sun, Y.; Du, J. Crystalline gallium oxide nanowires: Intensive blue light emitters. *Chem. Phys. Lett.* **2000**, *328*, 5–9. [[CrossRef](#)]
19. Binet, L.; Gourier, D. ORIGIN OF THE BLUE LUMINESCENCE OF β-Ga<sub>2</sub>O<sub>3</sub>. *J. Phys. Chem. Solids* **1998**, *59*, 1241–1249. [[CrossRef](#)]

20. Rodríguez, C.I.M.; Álvarez, M.; Ángel, L.; Rivera, J.D.J.F.; Arízaga, G.G.C.; Michel, C.R.  $\alpha$ -Ga<sub>2</sub>O<sub>3</sub> as a Photocatalyst in the Degradation of Malachite Green. *ECS J. Solid State Sci. Technol.* **2019**, *8*, Q3180–Q3186. [[CrossRef](#)]
21. Zhao, B.X.; Li, X.; Yang, L.; Wang, F.; Li, J.C.; Xia, W.X.; Li, W.J.; Zhou, L.; Zhao, C.L.  $\beta$ -Ga<sub>2</sub>O<sub>3</sub> nanorod synthesis with a one-step microwave irradiation hydrothermal method and its efficient photocatalytic degradation for perfluorooctanoic acid. *Photochem. Photobiol.* **2015**, *91*, 42–47. [[CrossRef](#)] [[PubMed](#)]
22. Jin, S.; Lu, W.; Stanish, P.C.; Radovanovic, P.V. Compositional control of the photocatalytic activity of Ga<sub>2</sub>O<sub>3</sub> nanocrystals enabled by defect-induced carrier trapping. *Chem. Phys. Lett.* **2018**, *706*, 509–514. [[CrossRef](#)]
23. Wang, Y.; Li, N.; Duan, P.; Sun, X.; Chu, B.; He, Q. Properties and Photocatalytic Activity of  $\beta$ -Ga<sub>2</sub>O<sub>3</sub> Nanorods under Simulated Solar Irradiation. *J. Nanomater.* **2015**, *2015*, 126.
24. Minami, T. Oxide thin-film electroluminescent devices and materials. *Solid-State Electron.* **2003**, *47*, 2237–2243. [[CrossRef](#)]
25. Ji, Z.; Du, J.; Fan, J.; Wang, W. Gallium oxide films for filter and solar-blind UV detector. *Opt. Mater.* **2006**, *28*, 415–417. [[CrossRef](#)]
26. Oshima, Y.; Vllora, E.G.; Shimamura, K. Quasi-heteroepitaxial growth of  $\beta$ -Ga<sub>2</sub>O<sub>3</sub> on off-angled sapphire (0001) substrates by halide vapor phase epitaxy. *J. Cryst. Growth* **2015**, *410*, 53–58. [[CrossRef](#)]
27. Pawar, S.; Pawar, B.; Kim, J.; Joo, O.-S.; Lokhande, C. Recent status of chemical bath deposited metal chalcogenide and metal oxide thin films. *Curr. Appl. Phys.* **2011**, *11*, 117–161. [[CrossRef](#)]
28. Zainelabdin, A.; Zaman, S.; Amin, G.; Nur, O.; Willander, M. Deposition of well-aligned ZnO nanorods at 50 °C on metal, semiconducting polymer, and copper oxides substrates and their structural and optical properties. *Cryst. Growth Des.* **2010**, *10*, 3250–3256. [[CrossRef](#)]
29. Errico, V.; Arrabito, G.; Plant, S.R.; Medaglia, P.G.; Palmer, R.E.; Falconi, C. Chromium inhibition and sizeselcted Au nanocluster catalysis for the solution growth of lowdensity ZnO nanowires. *Sci. Rep.* **2015**, *5*, 12336. [[CrossRef](#)]
30. Arrabito, G.; Errico, V.; Zhang, Z.M.; Han, W.H.; Falconi, C. Nanotransducers on printed circuit boards by rational design of highdensity, long, thin and untapered ZnO nanowires. *Nano Energy* **2018**, *46*, 54–62. [[CrossRef](#)]
31. Zhao, Y.; Frost, R.L.; Yang, J.; Martens, W.N. Size and Morphology Control of Gallium Oxide Hydroxide GaO(OH), Nano- to Micro-Sized Particles by Soft-Chemistry Route without Surfactant. *J. Phys. Chem. C* **2008**, *112*, 3568–3579. [[CrossRef](#)]
32. Huang, C.-C.; Yeh, C.-S.; Ho, C.-J. Laser Ablation Synthesis of Spindle-like Gallium Oxide Hydroxide Nanoparticles with the Presence of Cationic Cetyltrimethylammonium Bromide. *J. Phys. Chem. B* **2004**, *108*, 4940–4945. [[CrossRef](#)]
33. Yao, J.; Wang, C. Decolorization of Methylene Blue with TiO<sub>2</sub> Sol via UV Irradiation Photocatalytic Degradation. *Int. J. Photoenergy* **2010**, *2010*, 643182. [[CrossRef](#)]

